2.6 High-Resolution X-ray Scattering

The high-resolution x-ray scattering program is focused on developing x-ray optics and applications: in particular, nuclear resonant scattering, inelastic x-ray scattering**,** and the application of high-resolution x-ray scattering techniques to fundamental measurements. *Inelastic nuclear resonant scattering* allows direct determination of partial phonon density of states in samples containing a suitable isotope with a low-energy nuclear transition. *Inelastic x-ray scattering*, on the other hand, enables measurement of phonon dispersion relations and form factors in single crystals and liquids. The emphasis in nuclear resonant scattering is developing unique applications, as this technique is more advanced in its instrumentation development. The emphasis in inelastic x-ray scattering is more on spectrometer development, in terms of resolution, throughput, and accuracy. The fundamental measurements are related to in-depth analysis of normal incidence diffraction, absolute wavelength measurements, and analysis of radiation from rotating frames, in the long pursuit of μeV-resolved spectroscopy.

2.6.1 Nuclear Resonant Scattering

Phonon-assisted nuclear resonant scattering of synchrotron radiation is a method originally developed by the group in 1995 (Sturhahn et al., 1995), following the successful development of meV resolution, tunable monochromators (Toellner et al., 1992; Mooney et al., 1994). With the availability of the 3-ID undulator beamline, the group continued to improve the method, by first reducing the energy resolution to under 1 meV (Toellner et al., 1997), and then applying it to samples under extreme *high pressure*, to *thin films and multilayers*, and to *biological systems*.

These applications are chosen based on their scientific merit, the unique nature of inelastic nuclear resonant scattering, or because other established methods in particular areas can be considered limited.

2.6.1.1 High-pressure applications

Properties of materials change drastically under high pressure. In particular, accurate knowledge of the equation of state of iron under high pressure has special importance in geophysics, since iron is the dominant component in the earth's core.

In collaboration with Geophysical Laboratories of the Carnegie Institute of Washington, the high-pressure group at the University of Paderborn, Germany, and the GSE-CARS-CAT of The University of Chicago, we have developed the necessary technology to measure phonon density of states under high pressure. The x-rays must be focused to a size smaller than 5 microns in diameter, and multiple avalanche photodiode (APD) detectors need to be mounted a few millimeters from the sample for a large solid-angle coverage. The final setup, shown in Fig. 2.46, incorporated a Kirkpatrick-Baez mirror system (Eng et al., 1998), a modified diamond anvil high-pressure cell, and three modified APD detectors. This is a permanent setup, placed in the 3-ID-B station for outside users.

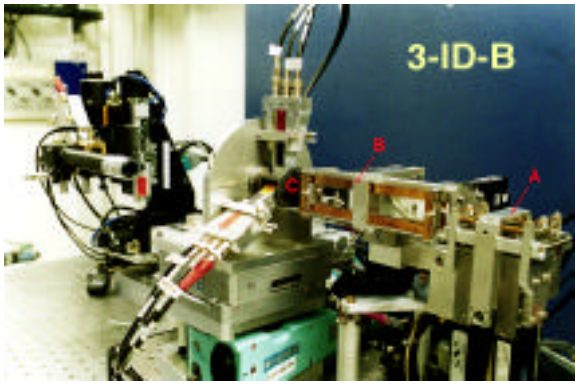

Fig. 2.46. The high-pressure setup in station 3-ID-B. Vertical (A) and horizontal (B) focusing mirrors in Kirkpatrick-Baez geometry reduce the beam size to under 5 microns in diameter. The diamond anvil cell is specially designed to accommodate three avalanche photodiode detectors (C), providing a 40% solid angle coverage. Very small samples of the order of several nanograms are sufficient.

The experiments were carried out for pure iron metal and wustite (FeO). The highest pressure reached is 153 GPa. Previous measurements that provided parameters for the equation of state were limited to 42 GPa.

From the data shown in Fig. 2.47, one can also extract model-free vibrational kinetic energy, zero-point energy, heat capacity, entropy, and Debye temperature (Mao et al., submitted) (see Fig. 2.48). Furthermore, using the Debye-like low-energy region of the excitation spectrum between 2-13 meV, it is possible to extract phonon velocities, which in turn, allow determination of bulk and shear moduli. This study shows that it is possible to measure complete elastic parameters up to pressures reaching that of earth's outer core. The elastic, thermodynamic, and energy parameters are essential for interpretation of seismological

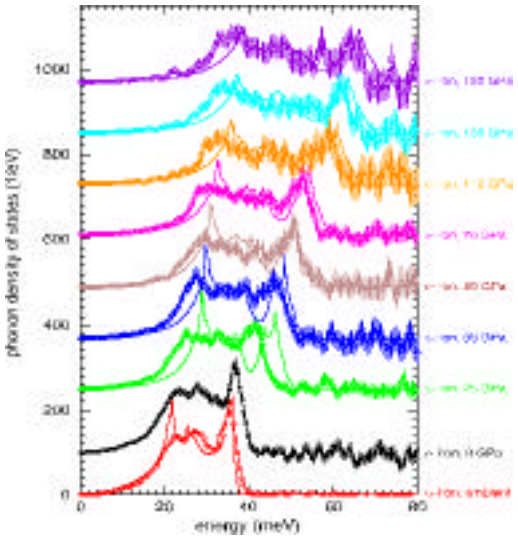

Fig. 2.47. The phonon density of states of Fe under high pressure. The solid lines are ab initio theoretical calculation (Toellner et al., 1997). The data were taken with 2 meV resolution.

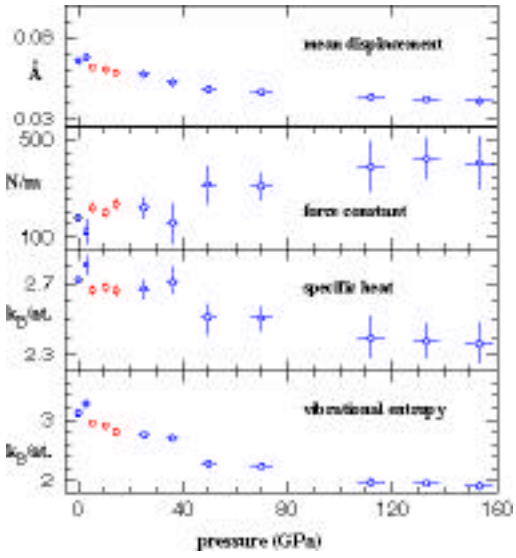

Fig. 2.48. The derived dynamical properties of iron metal as a function of pressure. The red data points are taken with a pressure medium to insure isotropic distribution.

observations and for numerical modeling of planetary cores.

One critical aspect of these measurements is the resolution function. The sharper the resolution function, both in terms of width and tails, the more reliable is the extraction of phonon velocities. Currently, the lowest possible resolution function with practical flux for measurements is 0.66 meV at the 14.4 keV ^{57}Fe nuclear transition. However, this 2-bounce monochromator is not compatible with microfocusing optics. A new type, 4-bounce nested monochromator, consisting of a novel mechanical concept called "artificial channel-cut" is being developed by the XFD synchrotron radiation instrumentation engineering group (Shu et al., submitted). Following the first successful implementation of this concept at 21.6 keV, we are now ready to build a 1 meV, in-line geometry monochromator to improve the quality of these experiments at 14.4 keV for ^{57}Fe and at 23.88 keV for the ^{119}Sn nuclear resonance.

The high-pressure measurements have also been extended to the ^{119}Sn isotope with an energy resolution of 1 meV at 23.88 keV (Fig. 2.49).

Improvements in monochromatization bandpass are considered to be a high priority. Along this line, the energy bandpass at 23.880 keV ^{119}Sn nuclear resonance has been further reduced to 0.5 meV by using two dispersive Si (12 12 12) crystals. The result, shown in Fig. 2.50 indicates that, as the resolution improves, the low dispersion points become more visible, thus providing even more stringent tests for the theoretical models and calculations.

The methodology for ^{119}Sn was developed as part of the PhD thesis of Dr. Michael Hu (Hu, 1999; Hu et al., 1999a; Hu et al., 1999b).

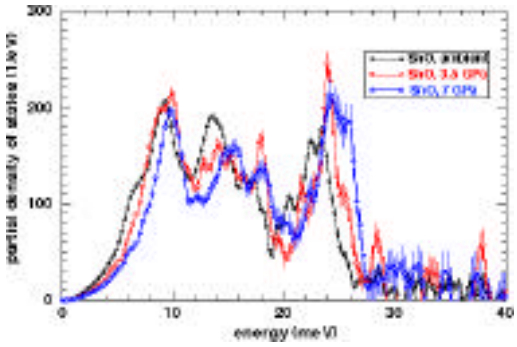

Fig. 2.49. The partial phonon density of states of SnO, measured up to 7 GPa with 1 meV overall resolution.

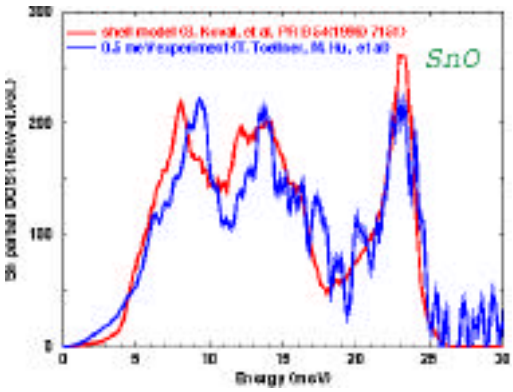

Fig. 2.50. The partial phonon density of states of SnO measured with 0.5 meV resolution and compared to the published result (Koval et al., 1996; Toellner, 2000).

2.6.1.2 Biological materials and organic molecules: Dynamics of proteins

X-ray scattering techniques have provided valuable information to understand the structure of biological systems. While diffraction techniques provide static information at the interatomic distance level and small angle scattering is used to learn about the intermediate range order, the dynamical information is limited to Debye-Waller factors. The "snap-shot" experiments provide nanosecond-resolved structural information. However, full dynamical information requires knowledge about the vibrational frequencies and dispersion of collective modes. The relationship between folding chains and active centers is an important part of the function of proteins. In this context, inelastic nuclear resonant scattering may play an important role as Fe is at the center of the heme group of protoporphyrin and acts as a binding site for O_2, CO, and H_2O.

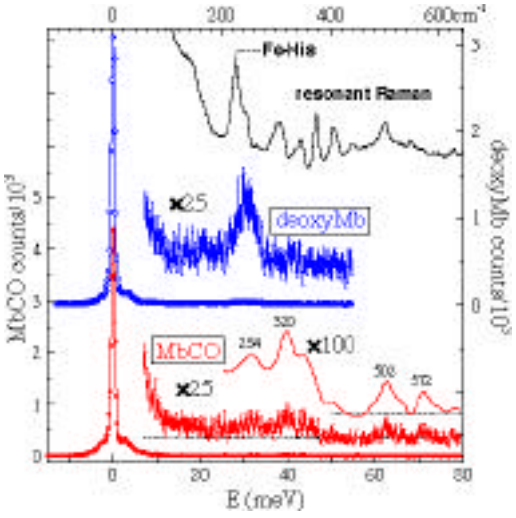

Fig. 2.51. The effect of CO on heme-group vibrations measured by inelastic nuclear resonant scattering.

Application of the nuclear resonant inelastic x-ray scattering (NRIXS) technique to biological materials with resonant isotopes at positions that are functionally important is very promising. In fact, NRIXS is the only method to provide reliable information below ~ 10 meV about such biologically active centers. The opportunity for systematic investigation of vibrational dynamics of biomolecules was realized at beamline 3-ID. We initiated outside collaborations [with T. Sage (Northeastern University), S. Durbin (Purdue University), and F. Parak and K. Achterhold (Technical University of Munich)] and initial experiments involve the oxygen-storing protein myoglobin (Mb). The NRIXS spectra of MbCO and deoxy-Mb are shown in Figs. 2.51 and 2.52. An energy resolution of 0.85 meV permits reliable determination of excitations down to ≈ 2 meV. In this experiment, the protein was

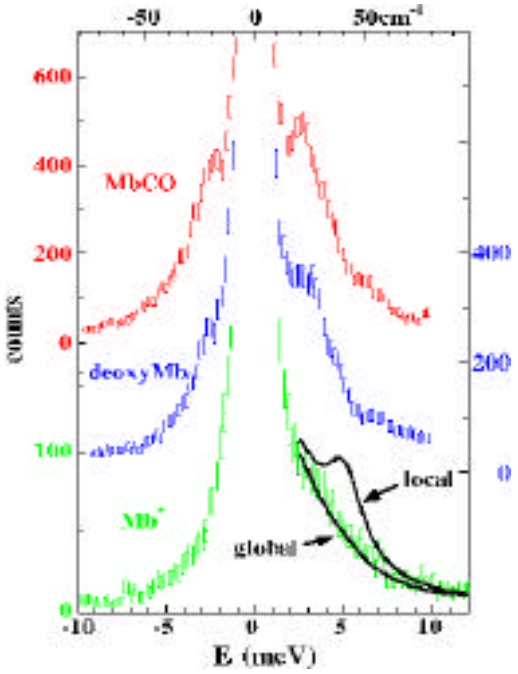

Fig. 2.52. The influence of CO ligation on the lower frequency heme vibrations.

solved in glycerol. The ^{57}Fe concentration was merely 7-10^{-5}.

In addition to NRIXS measurements, the technique of nuclear forward scattering provides unique data about interval fields and relaxation effects in the sub-meV regime (Keppler et al., 2000). The collaboration with Dr. T. Sage (Northeastern University) and Dr. S. Durbin (Purdue University) is focused on the photolysis of CO in myoglobin and on the properties of standard compounds (Sage et al., unpublished). The 3-ID beamline is the only place in any synchrotron radiation facility that has the resolution and the flux necessary to carry out such measurements at the present time.

2.6.1.3 Thin films, multilayers, and amorphous materials

The investigation of vibrational dynamics of thin films or multilayer structures has been traditionally difficult. In particular, excitation with larger momentum transfer (i.e., light scattering is not applicable), was almost inaccessible. NRIXS provides a unique solution to this situation.

The effect of confining a light element with a heavy element in a multilayer structure was studied in a Fe-Au multilayer structure, prepared in collaboration with the thin film group of the Materials Science Division of ANL (S. Bader, E. Fullerton, M. Grismdtich, and H. Sowers) and was characterized by various methods. The result is shown in Fig. 2.53.

The capability of NRIXS for determination of local phonon density of states (DOS) was demonstrated by measurements of ^{57}Fe monolayers deposited at the interface or interior of a ^{57}FeCr multilayer (Keune and Sturhahn, 1999) (see Fig. 2.54). In the Fe-Au system, we observe a pronounced softening of the vibrational modes with decreasing

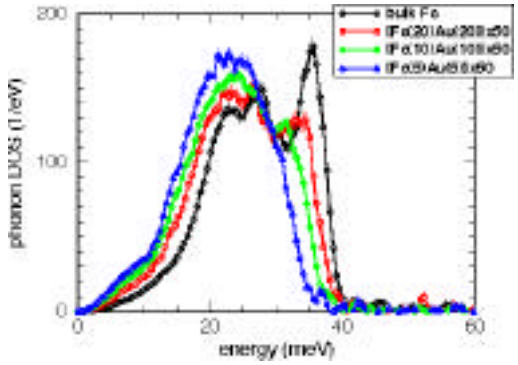

Fig. 2.53. The iron phonon density of states for Fe/Au multilayers with varying thickness. The x-ray diffraction and conversion electron Mössbauer spectroscopy results indicated that the Fe layers remain intact and magnetic, while the dynamical properties are changed drastically.

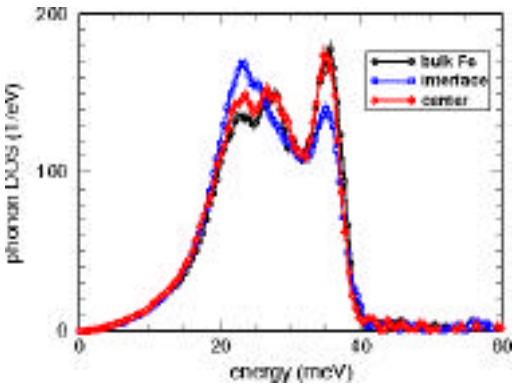

Fig. 2.54. The isotopic selectivity of nuclear resonant scattering is demonstrated in this experiment. The ^{57}Fe minelayer is selectively deposited either at the center of ^{56}Fe or at the Fe/Cr interface. When combined with nuclear forward scattering, it is possible to obtain chemical, magnetic, and dynamic behavior at the same time.

thickness of the Fe layers. Modes around 36 meV that are very strong in bcc Fe, almost completely disappear at the expense of excitations around 23 meV in the multilayer. The effects in the FeCr are subtler. The same principal behavior is observed at the interface; however, if the ^{57}Fe tracer layer is placed in the center of the ^{56}Fe layers, the DOS is almost identical to that of bcc iron. We also note a slight shift at the high-energy end of the spectrum. This technique is also applied to amorphous thin films as shown in Fig. 2.55.

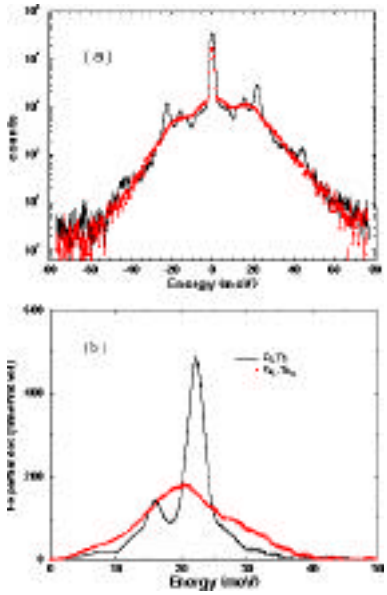

Fig. 2.55. The effect of crystalline-amorphous phase transition on phonon density of states in a Fe_2Tb alloy. The raw data clearly indicate the two-phonon contributions around 40 meV, as well as the quality of the signal over 5 decades.

2.6.2 Inelastic X-ray Scattering

2.6.2.1 A new spectrometer with 2 meV resolution for inelastic x-ray scattering

X-ray scattering with an energy resolution of a few meV provides a tool for investigating phonon excitations in condensed matter. In contrast to inelastic neutron scattering, there are virtually no limitations in the accessible energy-momentum space arising from the mass of the probe. In particular, for non-crystalline matter, this is an important advantage, because the collective dynamics has to be investigated at low momentum transfers and high energy transfers, a region difficult to access with conventional neutron scattering. Experiments at the European Synchrotron Radiation Facility (ESRF) with inelastic x-ray scattering on liquid and amorphous samples have attracted considerable attention during the past five years (see, e.g., measurements on liquid water by Sette et al., 1995; and on liquid lithium by Sinn et al., 1997).

The new spectrometer at station 3-ID-C is a state-of-the-art instrument that allows one to perform inelastic measurements with comparable or superior flux and resolution compared to the ESRF spectrometers. The monochromatization at 21.657 keV is achieved by a combination of a water-cooled diamond high-heat-load monochromator and an in-line monochromator that consists of two nested channel-cut crystals (Fig. 2.56).

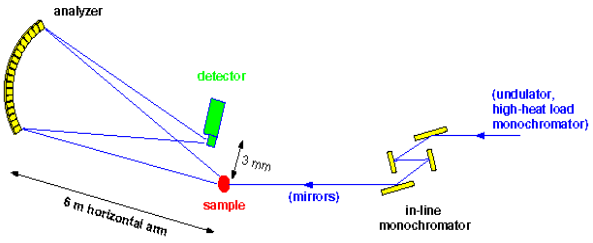

Fig. 2.56. Inelastic spectrometer at station 3-ID-C.

Development of the outer channel-cut of the monochromator, a so-called artificial channel-cut, allows one to adjust the two crystals with a mechanical precision of a few nanoradians with respect to each other.

The energy transmitted through the monochromator can be varied in a range up to about 100 eV by rotating the two channel-cuts. The flux at the sample is 3×10^8 photons/sec in a spot size of 150 μm × 150 μm.

For the energy analysis, the (18,6,0) reflection of a spherically bent silicon disk was used in backscattering geometry (θ_{Bragg}= 89.98°) at about 6 m from the sample. In order to avoid bending stress, the silicon is diced into 1 mm large pieces. The radiation from the analyzer is collected by a semiconductor (Cd-Zn-Te) detector developed for backscattering geometry.

In order to change the scattering angle at the sample, the analyzer and detector have to be rotated around the sample. To achieve this, the analyzer is mounted on a 2-m-long x-z-slide, which can position the analyzer. The detector is rotated independently. To maintain the backscattering alignment, an optical feedback system is applied.

Within the geometrical limitation of the hutch, a maximum scattering angle of 15 degrees is possible, which corresponds to a maximum momentum transfer of about 3 $Å^{-1}$. An extension to 5 $Å^{-1}$ is possible by deflecting the beam before the sample with a germanium (111) reflection in the horizontal scattering plane. The loss of intensity due to this extra reflection is about 30%.

Commissioning of the 2 meV spectrometer

The energy resolution of the spectrometer can be determined by measuring the energy width, if (ideally) a pure elastic scatterer is used as a sample. In a good approximation, Plexiglas® at the structure factor maximum (1 $Å^{-1}$) can be used as such a sample. An energy scan with a 10 mm thick Plexiglas® sample revealed an energy width of 2.2 meV (see Fig. 2.57).

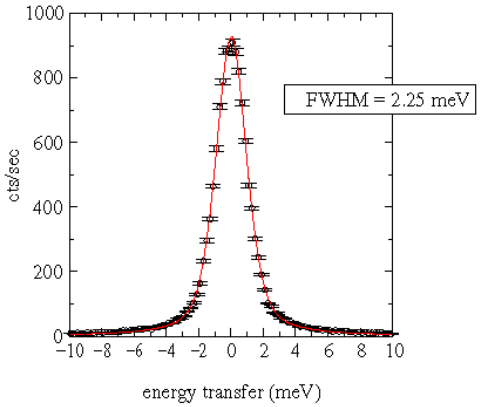

`

Fig. 2.57. Overall resolution function of the spectrometer.

To determine the accuracy of the energy scale, we measured phonon dispersion curves in a single crystal of beryllium. In Fig. 2.58, individual energy scans at different ζ values are shown. The position of the phonon peaks at ω≠0 yields the phonon dispersion for a particular phonon branch. The dispersions for the LA-TA and the LO-TO branches are shown in Fig. 2.59 and compared to literature from neutron experiments. The agreement is excellent and the deviations between the x-ray and neutron data are ≤ 2%, close to the statistical error of the data (Sinn et al., submitted).

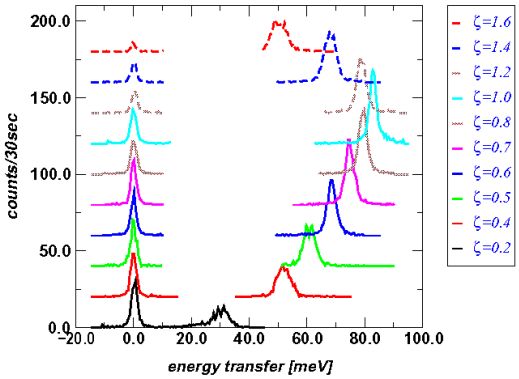

Fig. 2.58. Energy scans at different momentum transfers in a beryllium single crystal.

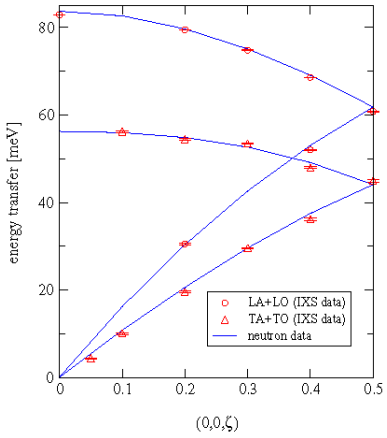

Fig. 2.59. Phonon dispersion in beryllium.

2.6.2.2 Inelastic x-ray measurements on liquid aluminum

Collective excitations in liquids have been extensively investigated in the recent years both experimentally and theoretically (see, e.g., Balucani and Zoppi, 1994). One characteristic feature of the collective excitations is the so-called positive dispersion, an increased slope in the dispersion relation compared to the macroscopic sound velocity. In alkaline metals this effect is of the order of 10-20% and can be explained by a viscoelastic shear modulus at high frequencies. In liquid water, however, a positive dispersion of more than twice the macroscopic sound velocity is observed (Sette et al., 1995); understanding the magnitude of this effect is still the subject of discussions. In one theoretical paper (Balucani et al., 1993), the authors suggest that the positive dispersion in water has the same origin as that in alkaline metals but is enlarged due to the high Einstein frequency in water. In liquid aluminum, the Einstein frequency is between those of the liquid alkaline metals and water, and therefore the magnitude of the enlargement of the sound velocity is expected to be in between water and the alkaline metals. Until now, no experimental data existed to check this hypothesis quantitatively.

We measured liquid aluminum at slightly above the melting point (at 1000°C) in a range of momentum transfers between 0.2 $Å^{-1}$ and 1.4 $Å^{-1}$. The preliminary results of the normalized intensity spectra S(Q,ω) are shown in Fig. 2.60. By transforming the data to the current-current correlation function

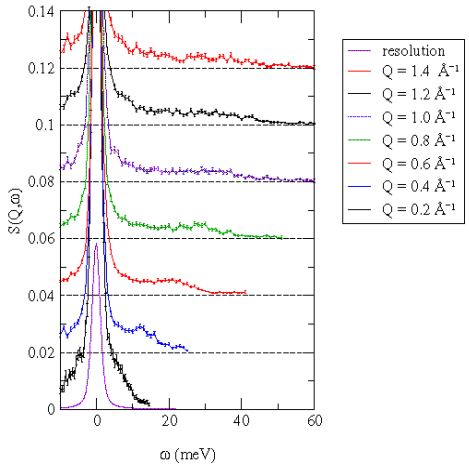

Fig. 2.60. Inelastic spectra for liquid aluminum for different momentum transfers.

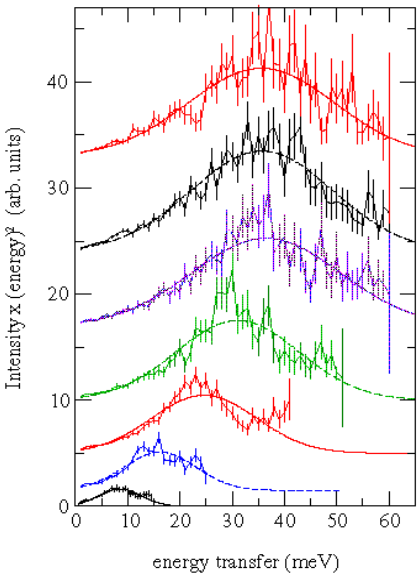

Fig. 2.61. Current-current correlation functions for the spectra shown in Fig. 2.60.

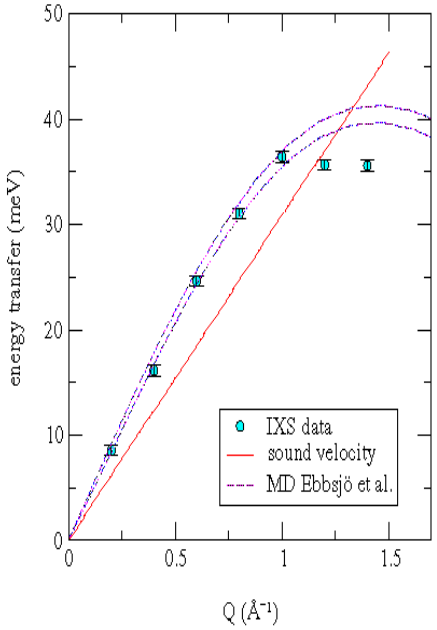

Fig. 2.62. Dispersion of the collective modes in liquid aluminum, derived from the current-current correlation function.

$C(Q,\omega) = \omega^2 S(Q,\omega)$, one can extract a dispersion relation (Figs. 2.61 and 2.62). A strong positive dispersion is observed, which also coincides with findings from computer simulations (Ebbsjoe et al., 1980). A further analysis of the data will reveal a more quantitative determination of the positive dispersion and of the damping of the modes (Sinn et al., submitted).

2.6.2.3 Investigation of collective excitation in lithium-ammonia mixtures

Solutions of alkali metals in ammonia have been investigated for over a century due to their many interesting properties. In these systems the outermost electron of the alkali metal separates from the ion, resulting in a free electron and an alkali metal ion. By variation of the metal concentration, one can change the electronic state of the system from an insulator to a liquid metal.

We performed measurements in a saturated solution of lithium in ammonia, where the system is a good metal. Energy scans at different momentum transfers are shown in Fig. 2.63. The curve at the bottom shows the resolution function of the spectrometer. As visible already in these raw data, there is a strong variation of the shape of the spectra with increasing momentum transfer. This is an indication for a collective mode dispersing at low momentum transfer with a speed close to the macroscopic sound velocity but also showing a strong softening around two times the Fermi momentum k_f for this system. This phenomenology is completely different than in pure ammonia. Rather than viewing the lithium–ammonia system as a incoherent mixture, stable complexes are most likely forming that consist of one lithium-atom surrounded by four ammonia atoms and that vibrate as one unit.

The surprisingly narrow width of these collective modes and their existence to relatively high momentum transfers suggests that the effective pair potentials between two complexes is close to a harmonic potential. A possible explanation for this unique experimental finding is that the size of the ammonia-lithium complexes coincides almost with half of the Fermi wavelength for this lithium concentration (Burns et al., unpublished).

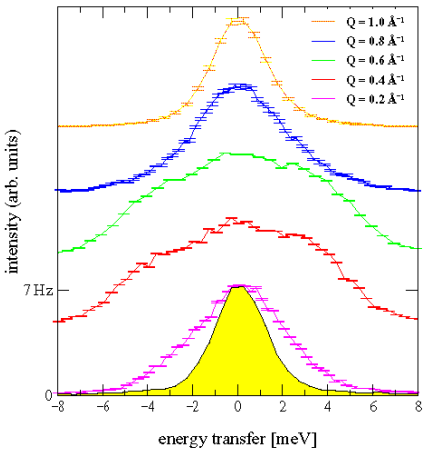

Fig. 2.63. Energy scans in a lithium-ammonia mixture for different momentum transfers.

2.6.3 Fundamental Measurements

2.6.3.1 Normal incidence diffraction in Si and Al_2O_3

High-resolution x-ray scattering takes advantage of special properties of crystals when the Bragg angle is near or at 90°, thus diffracting the beam practically onto itself. It is well known that the energy bandpass reaches its minimum value, while the angular acceptance is at its maximum. Multiple beam diffraction also accompanies the back-diffracted beam. Since this particular geometry is used for monochromatization and energy analysis, a detailed study was carried out, as part of Dr. John Stutter's thesis under joint supervision with Prof. R. Collela of Purdue University (Sutter, 2000). For silicon, with the exception of the Si (111) and (220) reflections, there is no multiple-beam free diffraction at 90 degrees. We have studied Si (12 4 0) and Si (18 6 0) in detail, since these are relevant energies for the ongoing programs.

The key ingredients for studying the multiple beam diffraction at normal incidence were the development of the milli-eV-resolved, tunable incident beam and the n-beam computer program (developed by Collela and modified by Sutter). The striking aspect of these measurements is the reduced reflectivity near the 90° Bragg angle: in an angular region of 40 μrad, the reflectivity drops to the 2% level. The shape of the resolution function is also critical, which is close to a Lorentzian with wide tails. The schematic general description is given in Fig. 2.64, and measurements are shown in Fig. 2.65.

The results of these studies have serious implications for high-resolution mono-chromatization and analysis, as well as x-ray Fabry-Perot interferometers. In an attempt to improve the efficiency of the diffracted beam, we have tried to identify other crystals with lower symmetry. It was suggested earlier that Al_2O_3 might be a good candidate.

We have pursued this option in collaboration with Dr. Yuri Shvydko (University of Hamburg). Among a dozen crystals tested, the standard and high-purity HEMEX crystals obtained from Crystals Systems,

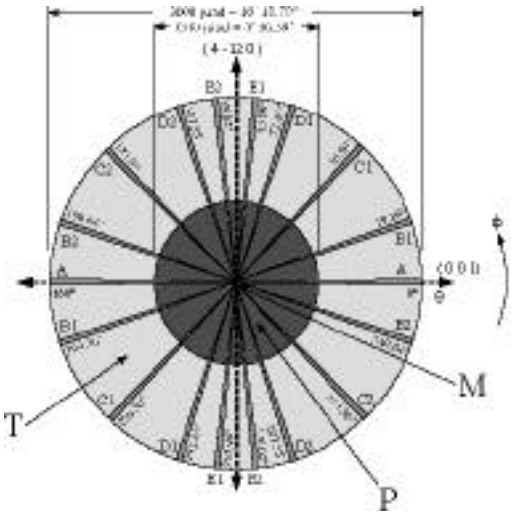

Fig. 2.64. A polar plot of all the multiple-beam cases occurring with Si (12 4 0) at 14.4381 keV. The angle ϕ is measured from the reciprocal lattice vector (001). The center of the plot is parallel to $-\boldsymbol{k}_0$ and antiparallel to the (12 4 0) vector. The distance from the center is proportional to the angle between $-\boldsymbol{k}_0$ and (12 4 0). The center region represents the strong 24-beam case close to exact backscattering. The letters A-E refer to conjugate pairs of reflections described in detail by Sutter et al. (in press).

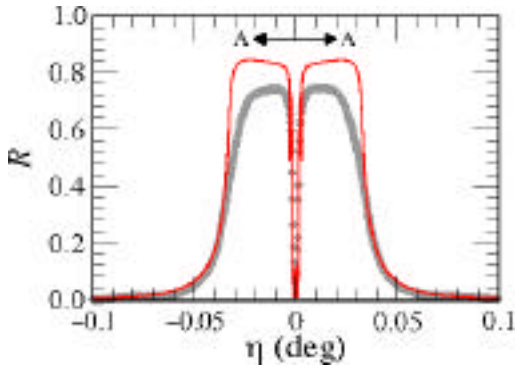

Fig. 2.65. Measured (gray) and calculated (red) reflec.6tivity of Si (12 4 0) at 14.438 keV measured under the normal incidence condition.

Inc., proved to have dislocation-free zones, and one of them gave the best result

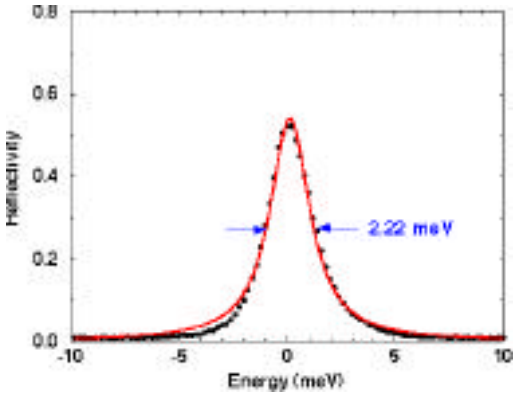

Fig. 2.66. The reflectivity of Al_2O_3 measured at 21.6306 keV, using a 1 meV bandpass incident beam. The Bragg angle is set to exactly 90°.

obtained to date, as shown in Fig. 2.66. The extinction depth for the Al_2O_3 (1 1 45) reflection is 133 μm. Therefore, dislocation-free crystals the size of the incident beam and a millimeter thick are necessary to have a good monochromator. Topographic investigations indicate a strong correlation between the dislocation density and reflectivity and resolution. These studies created the opportunity to realize the concept of exact backscattering proposed earlier.

2.6.3.2 X-ray wavelength standard

The narrow linewidth of some Mössbauer nuclei could be used as a length standard in the Angstrom scale, since they are easily reproducible with high accuracy. This wavelength is independent of temperature, pressure, and chemical condition of the sample at the part-per-trillion level. Prior to our measurements, the wavelength of the 14.4 keV Mössbauer transition of ^{57}Fe was known with an accuracy of 10 ppm: 14.413.00(15) eV (Bearden, 1965, 1967). The wavelength of ^{57}Fe Mössbauer radiation has now been determined with a relative

uncertainty of 0.19 ppm by using exact Bragg backscattering from a reference silicon crystal. The new value is 14.412497(3) eV. The new method takes advantage of the high brightness of the 3-ID beamline, with an undulator producing 14.4 keV radiation in the first harmonic (see Figs. 2.67 and 2.68).

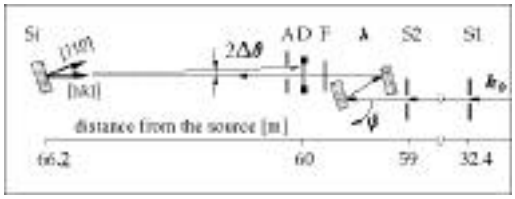

Fig. 2.67. The experimental setup. Slits S1 and S2 are set at 30 and 75 μm; λ: a λ-meter is a channel-cut Si monochromator whose temperature is kept constant within 2 mK and that is mounted on a Kohzu stage with 25 nrad resolution; F: an ^{57}Fe foil to provide Mössbauer radiation; D: a semitransparent APD detector; A: a 4 mm aperture to insure backscattering; and Si: the reference silicon crystal with a lattice constant of 5.43102030(36) Å.

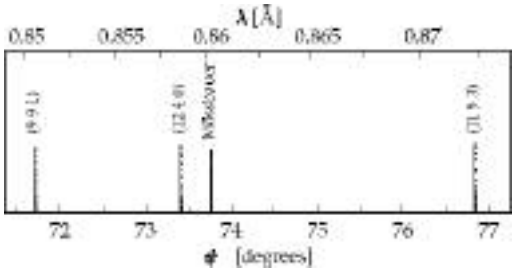

Fig. 2.68. Back-reflected and Mössbauer radiation in the detector plotted as a function of the angle of the wavelength-selecting monochromator λ, as shown in Fig. 2.67.

2.6.3.3 Instrumentation development

High-energy-resolution x-ray scattering experiments rely heavily on tunable, "in-line" crystal monochromators. When the resolution reaches 1 meV levels, the degree of asymmetry reaches near the Bragg angle, forcing the quality of the surface finish to be "mirror-like." Channel-cut single crystals are difficult to polish. In addition, a monochromatic x-ray beam delivered by a C (111) monochromator provides several millijoule power to the first face of the outer channel-cut crystal, causing a temperature difference of 100-200 mK compared to the second face of the same channel-cut. (The inside nested, higher order channel-cut crystal cuts down the energy bandpass from cV to meV level). Finally, geometrical restrictions dictated by crystal placement or allowable vertical offset makes simple-crystal channel-cut geometry impractical. These three unrelated difficulties can be overcome by separating the two faces of the outer channel-cut crystal and providing an artificial link between them. The mechanism described in section 3.3.4.4 was developed to solve this problem. The two separate crystals can be held together with better than 30 nrad angular stability, as shown in Fig. 3.28 (see section 3.3.4.4).